Multiphonon Fock state heralding with single-photon detection

Andrew J. Shepherd [*] and Ryan O. Behunin [†]
Department of Applied Physics and Materials Science, Northern Arizona University, Flagstaff, Arizona 86011, USA and Center for Materials Interfaces in Research and Applications (¡MIRA!), Flagstaff, Arizona, USA

(Received 25 July 2024; revised 26 November 2024; accepted 23 September 2025; published 20 October 2025)

Recognized as a potential resource for quantum technologies and a possible test bed for fundamental physics, the control and preparation of nonclassical states of mechanical oscillators have been explored extensively. Within optomechanics, quantum state synthesis can be realized by entangling photonic and phononic degrees of freedom followed by optical detection. Single-photon detection enables one of the most powerful forms of such heralded quantum state preparation, permitting the creation of single-phonon states when applied to conventional cavity optomechanical systems. As the complexity of optomechanical systems increases, single-photon detection may provide heralded access to a larger class of exotic quantum states. Here, we examine the quantum dynamics of optomechanical systems that permit forward Brillouin scattering, where a single-phonon mode mediates transitions between a collection of equally spaced optical resonances. Solving both the Schrodinger equation and the Lindblad master equation for this system, we find that initial states comprised of single photons or weak laser pulses evolve into complex quantum states where the frequency of single-photon states and the phonon occupation number are entangled. Physically, these interactions permit a single photon to scatter to lower frequencies, where phonon excitation occurs for each scattering event. Combining this result with frequency filtering, we show how single-photon detection can herald selected multiphonon Fock states, even in the presence of optical losses. We also present an approach for quantum tomography of the heralded phonon states, which in the form of a state swap from the phononic to photonic domain enables on-demand generation of multiphoton Fock states.

DOI: 10.1103/z8tj-ml6k

I. INTRODUCTION

Heralding techniques have proven to be a powerful tool for manipulating entangled quantum states. By measuring a component of an entangled system, it is possible to collapse the remainder of the system into a known quantum state. Single-photon detection is used extensively for these purposes, enabling, for example, the production of single photons via parametric down-conversion [1,2] and the preparation of photon-added coherent states [3]. Within the field of cavity optomechanics, heralded state preparation through single-photon detection has permitted the realization of single-phonon states [4,5]. Due to potentially long quantum coherence times [6–10] and large effective mass, such mechanical oscillators are promising candidates for applications in quantum information science, such as transducers [11,12], memories [13], repeaters [13], and sensors [14], as well as a test bed of fundamental physics [15–18]. However, advancing the applications mentioned above necessitates the development of systems and protocols that can access a wider variety of nonclassical phonon states [9,10,19,20].

Here, we examine the quantum dynamics of optomechanical systems that utilize forward Brillouin interactions for the first time. In sharp contrast with conventional backward Brillouin scattering [20], a single-phonon mode mediates interactions between neighboring resonances in a ladder of optical modes [21–23]. These dynamics are made possible in resonators (or highly confined waveguides), where the participating slow group velocity mechanical modes have (∼MHz–GHz) frequencies determined by the system geometry.

Taking the phonon to occupy the ground state initially, we solve the Schrodinger equation for a single-photon input, as well as for a weak laser input, i.e., small coherent state amplitude. We find that the scattering of the injected photon to lower frequencies corresponds to an increasing phonon occupation number, generating entangled states where the mode of single-photon occupation is correlated with the phonon occupation number. When combining this entanglement with single-photon detection of one of the resonant optical modes, our results present a path to heralded multiphonon Fock states. To investigate the heralded mechanical state, readout can be accomplished with balanced homodyne detection [3,24], made possible by swapping the multiphonon Fock state to the photonic domain with an optomechanical π pulse. Using the same state-transfer techniques, this system can facilitate on-demand generation of multiphoton Fock states [5].

II. FORWARD BRILLOUIN SCATTERING

Brillouin scattering involves inelastic light-matter interactions, where incident light will shift frequency upon interaction with acoustic phonons. The more commonly known backward Brillouin scattering involves two counterpropagating

[*]Contact author: as5262@nau.edu
[†]Contact author: ryan.behunin@nau.edu

Published by the American Physical Society under the terms of the Creative Commons Attribution 4.0 International license. Further distribution of this work must maintain attribution to the author(s) and the published article's title, journal citation, and DOI.

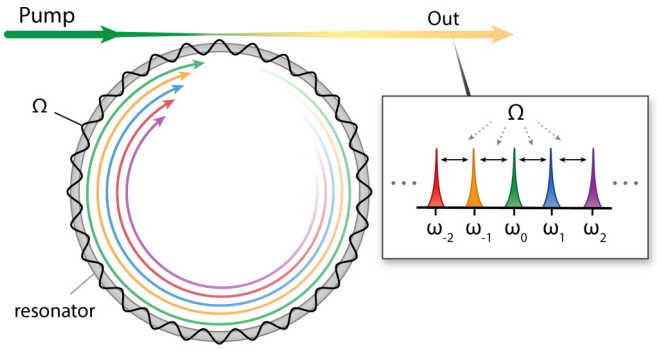

FIG. 1. Proposed FBS system, where a phonon, Ω, mediates transitions between a ladder of optical resonances in an optical resonator.

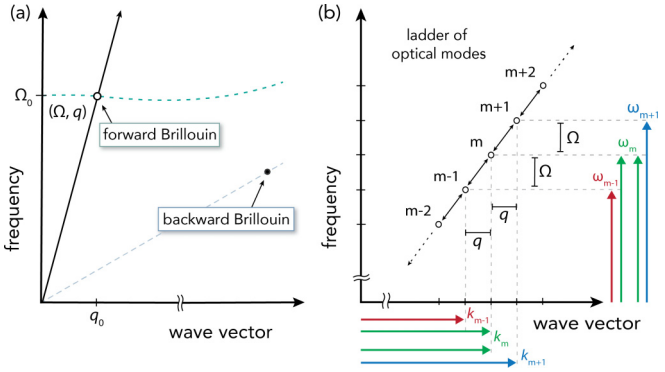

FIG. 2. Phase-matching conditions for intramodal forward Brillouin scattering in a resonator. (a) Acoustic dispersion, with the discrete forward Brillouin active mode shown as a white circle, where the mechanical frequency is approximately equal to the cutoff frequency, i.e., $\Omega \cong \Omega_0$. A backward Brillouin active mode is shown as a black dot for comparison. (b) Optical dispersion, where the phonon frequency and wave vector resonantly couple adjacent discrete optical modes.

light waves that can be coupled with a traveling sound wave via electrostriction [25]. Confined systems, such as resonators and waveguides, permit a form of forward Brillouin scattering (FBS) where a cutoff mechanical mode can transfer energy between copropagating optical resonances [21].

In FBS, this phonon mode with frequency Ω mediates scattering between a ladder of optical modes with frequencies labeled ω_m, where m is a general integer placeholder labeling each optical mode. This process is most efficient when the participating optical and mechanical waves satisfy phase-matching conditions, akin to energy and momentum conservation, given by

$$\omega_m = \omega_{m-1} + \Omega, \tag{1}$$

$$k_m = k_{m-1} + q, \tag{2}$$

where k_m and q are the wave vectors for the mth optical mode and phonon, respectively. Using the optical dispersion relation $\omega_m = ck_m/n_m$, where n_m is the effective index evaluated at ω_m, c is the speed of light, and noting that $k_{m-1} \approx k_m - (\omega_m - \omega_{m-1})\partial k_m/\partial\omega$, Eqs. (1) and (2) require that the phonon phase velocity is equal to the optical group velocity. While the phase velocity of sound is much less than light in bulk materials, Eqs. (1) and (2) can be satisfied in confined systems that support cutoff mechanical modes that can oscillate without propagating, i.e., $\Omega \neq 0$ when $q \approx 0$ (see Figs. 1 and 2).

Related systems comprising optical resonators that contain highly confined mechanical waveguides are suitable to realize FBS optomechanics when the mechanical frequency $\Omega/(2\pi)$ is an integer multiple of the optical free spectral range (FSR) (e.g., see Fig. 1). The Brillouin active mechanical mode for said systems is denoted in Fig. 2(a) as the white circle on the cutoff phonon dispersion curve. The optical dispersion and phase matching for these modes is shown in Fig. 2(b). While scattering to distant optical modes is physically limited by the optical dispersion, these effects are negligible for a broad variety of candidate systems over the relatively narrow frequency ranges of FBS [26]. For example, recent experiments demonstrate cascading to over 25 Stokes orders [27]. It is important to note that the dispersion curves in Fig. 2 would exhibit a continuum of allowable wave vectors for a linear waveguide. In addition, the following analysis assumes an optomechanical cavity system, whereas linear waveguide systems analytically require envelope operators [28].

In contrast with more familiar forms of Brillouin light scattering, FBS exhibits a phonon frequency and optomechanical coupling, which are highly tailorable with changes in the waveguide geometry, leading to selective resonant phonon frequencies and coupling strengths [23,29]. For example, tailored Brillouin shifts spanning 1–16 GHz have been experimentally demonstrated [30]. These properties have been explored in a broad variety of systems [31], including telecommunications [21], photonic crystal [32–35], and liquid-core [36] fibers; silicon waveguides [30,37,38]; microring [39] and microfluidic resonators [40]; and optical microspheres [41,42]. Forward scattering in these systems can be ensured as the dominant scattering mechanism when the Brillouin shift for backward scattering is not an integer multiple of the FSR of the optical cavity.

III. QUANTUM DYNAMICS

To model the quantum dynamics of an FBS optomechanical system, we use the Hamiltonian $H = H_0 + H_{\text{int}}$,

$$H_0 = \sum_{m=-\infty}^{\infty} \hbar(\omega_p + m\Omega)a_m^\dagger a_m + \hbar\Omega b^\dagger b, \tag{3}$$

$$H_{\text{int}} = \hbar g \sum_{m=-\infty}^{\infty} a_m a_{m-1}^\dagger b^\dagger + \text{H.c.}, \tag{4}$$

where H_0 and H_{int} describe the free evolution and interactions of the system, respectively, and H.c. denotes the Hermitian conjugate. Here, Ω, b, and $b^\dagger$ are the angular frequency, annihilation operator, and creation operator for the phonon mode, respectively. With ω_p as a central resonant frequency, the first term in H_0 describes the collection of resonantly spaced optical modes, where a_m is the annihilation operator for the mth optical mode that has the angular frequency $\omega_m = \omega_p + m\Omega$. As a consequence of the definition of ω_m, ideal phase matching is assumed throughout, i.e., $\omega_m = \omega_{m-1} + \Omega$. To reflect the independence of these distinct optical modes in the absence of FBS, the annihilation and creation operators satisfy

$[a_m, a^\dagger_{m'}] = \delta_{mm'}$ where $\delta_{mm'}$ is the Kronecker delta. The interaction Hamiltonian $H_{\rm int}$ and associated constant coupling rate g quantify the strength of forward Brillouin interactions that can be produced by electrostriction and radiation pressure [23,29]. Important conserved quantities that arise from the Hamiltonian include the noninteracting energy (H_0) and the total photon number ($\hat{N} = \sum_m a^\dagger_m a_m = \sum_m n_m$), given that $[H_0, H] = 0$ and $[\hat{N}, H] = 0$, where n_m is the number operator for the mth optical mode.

By considering dynamics occurring at times much shorter than reported phonon decoherence times, we neglect loss on the mechanical mode in our analytical model. This regime can be accessed when the Brillouin coupling rate exceeds the mechanical decoherence rate. As one example, forward Brillouin coupling rates as high as $g \sim (2\pi)29\,\text{kHz}$ and mechanical decoherence rates as low as $T_2^{-1} \sim (2\pi)1.2\,\text{kHz}$ have been realized in silicon systems, where the significant contribution is from dephasing [8,30,37]. We confirm this point by simulating the dynamics with physically realized phonon dephasing and loss values, seeing exceptional agreement with our analytical model. To first build intuition for the dynamics of this system, optical losses are neglected, but are later analyzed by solving the Lindblad master equation. Other than decreasing the probability of a heralding event, optical dissipation does not alter the essential conclusions of the lossless model.

An analytical solution of the system's lossless dynamics can be found through application of the time evolution operator on an initial state: $|\psi(t)\rangle = U(t,0)|\psi(0)\rangle$, with $U = \exp\{-iHt/\hbar\}$. Under the condition of phase-matched optical and mechanical modes, the FBS interaction described by $H_{\rm int}$ conserves energy (i.e., $[H_0, H_{\rm int}] = 0$), permitting the time evolution operator to be factorized in the following form:

$$U(t,0) = U_0 U_{\rm int}, \tag{5}$$

with $U_0 = \exp\{-iH_0 t/\hbar\}$ and $U_{\rm int} = \exp\{-iH_{\rm int}t/\hbar\}$. Taking advantage of the infinite discrete symmetry of the system [i.e., the involvement of an infinite ladder of equally spaced optical modes and constant coupling g in Eqs. (3) and (4)], $U_{\rm int}$ can be factored further using the Glauber formula, a special case of the Zassenhaus expansion,

$$e^{X+Y} = e^X e^Y e^{-\frac{1}{2}[X,Y]}, \tag{6}$$

where X and Y are placeholders for any operators satisfying $[X,[X,Y]] = 0$ and $[Y,[X,Y]] = 0$ [43]. For $U_{\rm int}$, the operators X and Y are given by

$$X = -igtAb^\dagger \quad \text{and} \quad Y = -igtA^\dagger b, \tag{7}$$

where

$$A = \sum_{m=-\infty}^{\infty} a_m a^\dagger_{m-1} \quad \text{and} \quad A^\dagger = \sum_{m=-\infty}^{\infty} a^\dagger_m a_{m-1}. \tag{8}$$

Noting that A and $A^\dagger$ commute,

$$[A, A^\dagger] = \sum_{m=-\infty}^{\infty}\sum_{m'=-\infty}^{\infty} [a_m a^\dagger_{m-1}, a^\dagger_{m'} a_{m'-1}] \tag{9}$$
$$= \sum_{m=-\infty}^{\infty} (n_{m-1} - n_m) = 0,$$

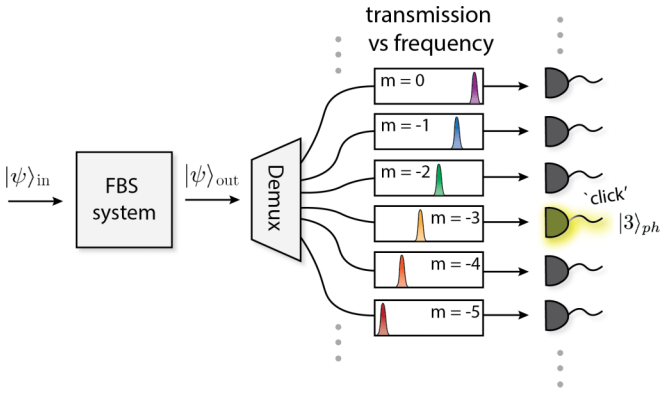

FIG. 3. Scheme describing quantum state synthesis in a forward Brillouin scattering system. The entangled state, $|\psi\rangle_{\rm out}$, goes through a demultiplexer, filtering by frequency into different transmission lines to an array of single-photon detectors. The detection event (shown by the yellow highlight) projects the phonon into a Fock state.

we find $[X,Y] = g^2t^2AA^\dagger$ and $[X,[X,Y]] = [Y,[X,Y]] = 0$, permitting application of the Glauber formula and leading to the factorized form of $U_{\rm int}$ given by

$$U_{\rm int} = e^{-igtAb^\dagger} e^{-igtA^\dagger b} e^{-\frac{1}{2}g^2t^2AA^\dagger}. \tag{10}$$

We assume that the phonon is initially found in the ground state. For standard dilution refrigerator systems, this assumption places constraints on the frequencies of the participating mechanical mode. For example, mechanical frequencies, $\Omega/2\pi$, exceeding 1 GHz provide >99.1% ground-state occupancy at 10 mK, frequencies and temperatures that are readily achieved [9,30,37]. Additionally, we consider a single photon injected into the $m = 0$ mode, providing an initial state of $|\psi(0)\rangle = |\ldots, 0_{-1}, 1_0, 0_1, \ldots\rangle \otimes |0\rangle_{\rm ph}$. Here, the first ket describes the ladder of optical modes with each mode separated by a comma and where the suffix labels the optical mode. The second ket describes the state of the phonon, i.e., $|0\rangle_{\rm ph}$. Explicit calculation of $U(t,0)|\psi(0)\rangle$ gives

$$|\psi(t)\rangle = e^{-i\omega_0 t} e^{-\frac{g^2t^2}{2}} \sum_{n=0}^{\infty} \frac{(-igt)^n}{\sqrt{n!}} |\varphi_n\rangle \otimes |n\rangle_{\rm ph}, \tag{11}$$

where we have introduced the compact notation

$$|\varphi_n\rangle = |\ldots, 0_{-n-1}, 1_{-n}, 0_{-n+1}, \ldots\rangle. \tag{12}$$

This entangled superposition state quantifies how the input photon is Stokes shifted in frequency down the resonant optical ladder while simultaneously increasing the occupation number of the phonon mode.

Equation (11) shows how measuring a photon of a specified frequency ω_j can collapse the wave function and isolate a highly nonclassical phonon quantum state. To achieve this, the quantum state is spatially entangled by demultiplexing the emitted optical state as a function of frequency, where subsequent single-photon detection in the $-j$th optical mode signals the collapse of the wave function into a phonon Fock state of known occupation number. An example of this heralding process is shown in Fig. 3, where $|\psi\rangle_{\rm in}$ is the injected photon and $|\psi\rangle_{\rm out}$ is the entangled state to be filtered by frequency into different transmission lines, leading

to single-photon detectors. Owing to the large optical spacing determined by Ω, the required demultiplexing is readily achieved in state-of-the-art, chip-scale filters [44,45]. In this example, the detected photon has been Stokes shifted to mode $m = -3$, corresponding to the generation of an $n = 3$ phonon Fock state.

Although permitting analytical simplicity, single-photon inputs present greater experimental challenges, requiring a heralding process to achieve the desired initial state. A more physically accessible initial state would be the input of a weak coherent state (faint laser), where the initial state of the $m = 0$ optical mode is given by $|\alpha\rangle \approx |0\rangle + \alpha|1\rangle$ ($|\alpha| \ll 1$), taking the place of $|\psi\rangle_{\text{in}}$ in Fig. 3. Applying the time evolution operator on $|\psi(0)\rangle \approx |\text{vac}\rangle \otimes |0\rangle_{\text{ph}} + \alpha|\varphi_0\rangle \otimes |0\rangle_{\text{ph}}$ gives the wave function at time t,

$$|\psi(t)\rangle \approx |\text{vac}\rangle \otimes |0\rangle_{\text{ph}} + \alpha e^{-i\omega_p t} e^{-\frac{g^2 t^2}{2}} \times \sum_{n=0}^{\infty} \frac{(-igt)^n}{\sqrt{n!}} |\varphi_n\rangle \otimes |n\rangle_{\text{ph}}, \tag{13}$$

with $|\text{vac}\rangle$ denoting vacuum for all optical modes. For this wave function, the vacuum state dominates in probability; however, the phonon manipulation relies on conditional measurement. While the detection probability is low, the entire state collapses upon detection, heralding a phonon Fock state in the same manner as before. Lower bounds on state synthesis fidelity, produced by corrections to the coherent state approximation above, are estimated in Sec. I of the Supplemental Material [46].

Having described the dynamics of the lossless system, we now analyze the effects of optical losses using the Lindblad master equation. When weakly coupled to a zero-temperature Markovian bath, the density matrix for the system satisfies

$$\dot{\rho} = -\frac{i}{\hbar}[H, \rho] + \frac{\gamma}{2} \sum_{m=-\infty}^{\infty} (2a_m \rho a_m^\dagger - a_m^\dagger a_m \rho - \rho a_m^\dagger a_m), \tag{14}$$

producing exponential decay for each optical mode at the decay rate γ [47]. Restricting our attention to single-photon input and accounting for losses modeled by Eq. (14), the density matrix can be represented by

$$\rho = \sum_{n,n'} [\alpha_{n,n'} |\varphi_n\rangle\langle\varphi_{n'}| + \beta_{n,n'} \delta_{nn'} |\text{vac}\rangle\langle\text{vac}|] \otimes |n\rangle_{\text{ph}}\langle n'|_{\text{ph}}, \tag{15}$$

where Eq. (14) provides the following equations for the time-dependent coefficients $\alpha_{n,n'}$ and $\beta_{n,n'}$:

$$\dot{\alpha}_{n,n'} = -ig(\sqrt{n}\alpha_{n-1,n'} + \sqrt{n+1}\alpha_{n+1,n'} - \sqrt{n'}\alpha_{n,n'-1} - \sqrt{n'+1}\alpha_{n,n'+1}) - \gamma\alpha_{n,n'}, \tag{16}$$

$$\dot{\beta}_{n,n'} = \gamma \delta_{nn'} \alpha_{n,n'}. \tag{17}$$

The solution to these two equations, given by

$$\alpha_{n,n'} = \frac{(-igt)^n (igt)^{n'}}{\sqrt{n!}\sqrt{n'!}} e^{-g^2 t^2 - \gamma t}, \tag{18}$$

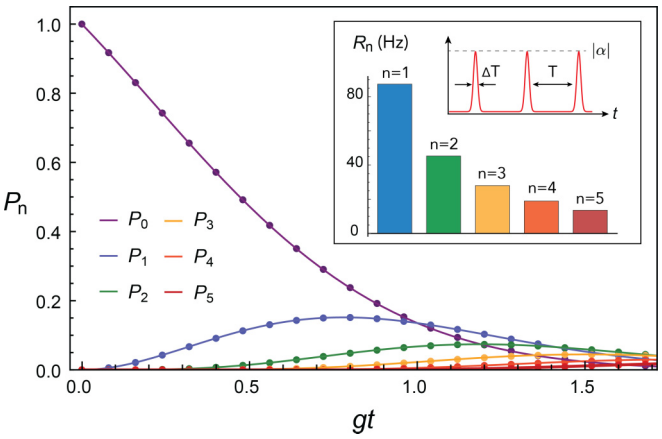

FIG. 4. Detection probabilities for the first few accessible states when FBS system is stimulated with a single photon, plotted over gt (g as the coupling rate, t as time). Optical loss is taken as $\gamma = g$. Solid lines correspond to Eq. (20) and circles correspond to simulations that include mechanical dephasing and loss. Inset: Heralding rates for Fock states $n = 1$–5 $|n\rangle_{\text{ph}}$ in Hz with pulsed source amplitude $|\alpha| = 0.2$ and duty cycle $T = 2/g$.

$$\beta_{n,n'} = \delta_{n,n'} \gamma \int_0^t d\tau \frac{(g\tau)^{2n}}{n!} e^{-g^2\tau^2 - \gamma\tau}, \tag{19}$$

can be shown to preserve the trace of the density matrix [i.e., $\text{tr}(\rho) = 1$], and gives the probability of single-photon detection in the $-j$th mode (i.e., $P_j = \alpha_{j,j}$) and collapse to a phonon Fock state of number j,

$$P_j = \frac{(gt)^{2j}}{j!} e^{-g^2 t^2 - \gamma t}. \tag{20}$$

This result shows that although the detection probability is suppressed by $\exp\{-\gamma t\}$, the entanglement between single-photon occupation and phonon Fock state is preserved. Thus, optical losses do not fundamentally alter the ability to herald complex phononic states (see Fig. 4 with $\gamma = g$ as solid lines).

Figure 4 also shows the impact of phonon losses and decoherence on the heralding probabilities. The circles represent simulated dynamics that include experimentally determined values for mechanical loss ($\sim$ Hz) and dephasing ($\sim$ kHz) [8], showing agreement with the analytical model. In this example, mechanical decoherence is dominated by dephasing, $T_2^{-1} \simeq \gamma_\phi$, which is modeled in the Lindblad master equation with the jump operator $\sqrt{\gamma_\phi} b^\dagger b$. While large γ_ϕ can impact the quantum evolution, pure dephasing does not change Hilbert space; i.e., phonon number and photon frequency remain correlated. Additionally, we find through simulation that the system's evolution is insensitive to increasing mechanical loss and dephasing by a few orders of magnitude (see Sec. II of the Supplemental Material [46]). We estimate the average heralding rates R_n for each phonon Fock state to range from 10 to 90 Hz when stimulated with a weak coherent state, where $|\alpha| = 0.2$. Here, $R_n \simeq |\alpha|^2 \overline{P_n}/T$, where T is the duty cycle of weak laser pulses and $\overline{P_n}$ is the heralding probability averaged over the T. The heralding rate is limited by T, which must be long enough to allow for significant quantum evolution and suppress the chance of double photon occupancy.

After the detection event, readout and manipulation of the phonon state can be done through optomechanical π and $\pi/2$ pulses [20], where a beam splitter interaction between phonons and photons can be realized by intense optical pulses. In an FBS system, enabling this requires engineered mode suppression on a resonant mode of higher frequency than the input photon, where the occupation is forbidden. Otherwise, an intense optical pulse will simultaneously lead to beam splitting and two-mode squeezing interaction. Leveraging that the injected photon cannot scatter to frequencies higher than $m = 0$, Eq. (11) satisfies the Schrodinger equation with a single-photon input for suppression of any mode $m = j > 0$. Suppression of mode ω_j removes the terms containing a_j or $a_j^\dagger$ from the sum in Eqs. (3) and (4), leaving only an anti-Stokes sideband for the ω_{j+1} mode. Thus, strong pulses with frequency ω_{j+1} can transfer or superpose the heralded mechanical states into or with the optical domain at ω_{j+2}, where they can be isolated using bandpass filters and analyzed with balanced homodyne detection [3,24], given that the swap operation occurs at times before thermal decoherence times ($\ll n^{-1}T_1$ for Fock state $|n\rangle$ at 20 mK [48]) after the heralding event. Physically, this mode suppression can be engineered in a multitude of ways, including structural changes to the resonator system [49–52] or Bragg gratings in linear waveguides [53,54].

In addition to verification of the nonclassical mechanical states, our findings indicate an approach to on-demand generation of multiphoton Fock states. Multiphoton states are a prerequisite for the synthesis of a variety of complex entangled states [55–58], which contribute to applications across quantum information processing [59–61]. Benefiting from long mechanical coherence times, an optomechanical π pulse can map a stored heralded phonon state to a photonic state in a well-defined spatial and spectral mode [5]. Although the heralding event is probabilistic, applying feedback techniques can approach near-deterministic generation [62,63].

In summary, we show how the quantum dynamics of intramodal spontaneous forward Brillouin scattering can be paired with single-photon detection to herald phonon Fock states of an arbitrary and selective number. Exploiting the entanglement generated by the system when stimulated with a single photon or a faint laser, single-photon detection collapses the mechanical state of definite phonon number, determined by the relative frequency shift of the detected photon with respect to the optical input. We discuss a method for quantum tomography via balanced homodyne detection of the mechanical-to-optical swapped quantum state, which by the same process suggests the use of these systems as an on-demand multiphoton source.

We have shown that mechanical decoherence can be neglected for times much shorter than the phonon lifetime, and although optical losses can be significant, a lost photon will only lower the probability of detection, leaving the heralded multiphonon Fock state unaffected. This result, in conjunction with long phonon quantum coherence times, the compatibility of these systems with telecommunication wavelengths of light, the large effective mass of the phonon modes, and access to a ladder of resonant frequencies of light, has the potential to enable new quantum devices, new approaches to state synthesis, and open new windows on fundamental physics questions.

ACKNOWLEDGMENTS

This work was supported by NSF Awards No. 2145724 and No. 2427169. The authors thank Peter Rakich, Shruti Puri, and Margaret Pavlovich for stimulating discussions.

DATA AVAILABILITY

All data supporting the findings of this study are given in the manuscript and its supplementary material. Additional data is available from the authors upon request.

[1] C. Couteau, Spontaneous parametric down-conversion, Contemp. Phys. **59**, 291 (2018).

[2] L. Caspani, C. Xiong, B. J. Eggleton, D. Bajoni, M. Liscidini, M. Galli, R. Morandotti, and D. J. Moss, Integrated sources of photon quantum states based on nonlinear optics, Light Sci. Appl. **6**, e17100 (2017).

[3] A. Zavatta, S. Viciani, and M. Bellini, Quantum-to-classical transition with single-photon-added coherent states of light, Science **306**, 660 (2004).

[4] S. Hong, R. Riedinger, I. Marinković, A. Wallucks, S. G. Hofer, R. A. Norte, M. Aspelmeyer, and S. Gröblacher, Hanbury Brown and Twiss interferometry of single phonons from an optomechanical resonator, Science **358**, 203 (2017).

[5] C. Galland, N. Sangouard, N. Piro, N. Gisin, and T. J. Kippenberg, Heralded single-phonon preparation, storage, and readout in cavity optomechanics, Phys. Rev. Lett. **112**, 143602 (2014).

[6] M. Goryachev, D. L. Creedon, E. N. Ivanov, S. Galliou, R. Bourquin, and M. E. Tobar, Extremely low-loss acoustic phonons in a quartz bulk acoustic wave resonator at millikelvin temperature, Appl. Phys. Lett. **100**, 243504 (2012).

[7] M. Goryachev, D. L. Creedon, S. Galliou, and M. E. Tobar, Observation of Rayleigh phonon scattering through excitation of extremely high overtones in low-loss cryogenic acoustic cavities for hybrid quantum systems, Phys. Rev. Lett. **111**, 085502 (2013).

[8] G. S. MacCabe, H. Ren, J. Luo, J. D. Cohen, H. Zhou, A. Sipahigil, M. Mirhosseini, and O. Painter, Nano-acoustic resonator with ultralong phonon lifetime, Science **370**, 840 (2020).

[9] K. J. Satzinger, Y. P. Zhong, H.-S. Chang, G. A. Peairs, A. Bienfait, M.-H. Chou, A. Y. Cleland, C. R. Conner, É. Dumur, J. Grebel, I. Gutierrez, B. H. November, R. G. Povey, S. J. Whiteley, D. D. Awschalom, D. I. Schuster, and A. N. Cleland, Quantum control of surface acoustic-wave phonons, Nature (London) **563**, 661 (2018).

[10] Y. Chu, P. Kharel, T. Yoon, L. Frunzio, P. T. Rakich, and R. J. Schoelkopf, Creation and control of multi-phonon Fock states in a bulk acoustic-wave resonator, Nature (London) **563**, 666 (2018).

[11] K. Stannigel, P. Rabl, A. S. Sørensen, P. Zoller, and M. D. Lukin, Optomechanical transducers for long-distance quantum communication, Phys. Rev. Lett. **105**, 220501 (2010).

[12] W. Jiang, C. J. Sarabalis, Y. D. Dahmani, R. N. Patel, F. M. Mayor, T. P. McKenna, R. Van Laer, and A. H. Safavi-Naeini, Efficient bidirectional piezo-optomechanical transduction between microwave and optical frequency, Nat. Commun. **11**, 1166 (2020).

[13] M. Pechal, P. Arrangoiz-Arriola, and A. H. Safavi-Naeini, Superconducting circuit quantum computing with nanomechanical resonators as storage, Quantum Sci. Technol. **4**, 015006 (2018).

[14] D. Mason, J. Chen, M. Rossi, Y. Tsaturyan, and A. Schliesser, Continuous force and displacement measurement below the standard quantum limit, Nat. Phys. **15**, 745 (2019).

[15] W. Marshall, C. Simon, R. Penrose, and D. Bouwmeester, Towards quantum superpositions of a mirror, Phys. Rev. Lett. **91**, 130401 (2003).

[16] L. Diósi, Models for universal reduction of macroscopic quantum fluctuations, Phys. Rev. A **40**, 1165 (1989).

[17] R. Penrose, On the gravitization of quantum mechanics 1: Quantum state reduction, Found. Phys. **44**, 557 (2014).

[18] G. C. Ghirardi, P. Pearle, and A. Rimini, Markov processes in Hilbert space and continuous spontaneous localization of systems of identical particles, Phys. Rev. A **42**, 78 (1990).

[19] Y. Chu, P. Kharel, W. H. Renninger, L. D. Burkhart, L. Frunzio, P. T. Rakich, and R. J. Schoelkopf, Quantum acoustics with superconducting qubits, Science **358**, 199 (2017).

[20] R. O. Behunin and P. T. Rakich, Harnessing nonlinear dynamics for quantum state synthesis of mechanical oscillators in tripartite optomechanics, Phys. Rev. A **107**, 023511 (2023).

[21] R. M. Shelby, M. D. Levenson, and P. W. Bayer, Resolved forward Brillouin scattering in optical fibers, Phys. Rev. Lett. **54**, 939 (1985).

[22] M. G. Raymer and J. Mostowski, Stimulated Raman scattering: Unified treatment of spontaneous initiation and spatial propagation, Phys. Rev. A **24**, 1980 (1981).

[23] P. Kharel, R. O. Behunin, W. H. Renninger, and P. T. Rakich, Noise and dynamics in forward Brillouin interactions, Phys. Rev. A **93**, 063806 (2016).

[24] A. Ourjoumtsev, R. Tualle-Brouri, and P. Grangier, Quantum homodyne tomography of a two-photon Fock state, Phys. Rev. Lett. **96**, 213601 (2006).

[25] Stimulated Brillouin and stimulated Rayleigh scattering, in *Nonlinear Optics*, edited by R. W. Boyd, 3rd ed. (Academic Press, Burlington, 2008), Chap. 9, pp. 429–471.

[26] C. Wolff, B. Stiller, B. J. Eggleton, M. J. Steel, and C. G. Poulton, Cascaded forward Brillouin scattering to all Stokes orders, New J. Phys. **19**, 023021 (2017).

[27] T. Shanavas, M. Grayson, B. Xu, M. Zohrabi, W. Park, and J. T. Gopinath, Cascaded forward Brillouin lasing in a chalcogenide whispering gallery mode microresonator, APL Photonics **7**, 116108 (2022).

[28] P. Rakich and F. Marquardt, Quantum theory of continuum optomechanics, New J. Phys. **20**, 045005 (2018).

[29] P. T. Rakich, C. Reinke, R. Camacho, P. Davids, and Z. Wang, Giant enhancement of stimulated Brillouin scattering in the subwavelength limit, Phys. Rev. X **2**, 011008 (2012).

[30] H. Shin, W. Qiu, R. Jarecki, J. A. Cox, R. H. Olsson, A. Starbuck, Z. Wang, and P. T. Rakich, Tailorable stimulated Brillouin scattering in nanoscale silicon waveguides, Nat. Commun. **4**, 1944 (2013).

[31] B. J. Eggleton, C. G. Poulton, P. T. Rakich, M. J. Steel, and G. Bahl, Brillouin integrated photonics, Nat. Photon. **13**, 664 (2019).

[32] M. S. Kang, A. Nazarkin, A. Brenn, and P. St. J. Russell, Tightly trapped acoustic phonons in photonic crystal fibres as highly nonlinear artificial Raman oscillators, Nat. Phys. **5**, 276 (2009).

[33] M. S. Kang, A. Brenn, and P. St. J. Russell, All-optical control of gigahertz acoustic resonances by forward stimulated interpolarization scattering in a photonic crystal fiber, Phys. Rev. Lett. **105**, 153901 (2010).

[34] W. H. Renninger, R. O. Behunin, and P. T. Rakich, Guided-wave Brillouin scattering in air, Optica **3**, 1316 (2016).

[35] W. H. Renninger, H. Shin, R. O. Behunin, P. Kharel, E. A. Kittlaus, and P. T. Rakich, Forward Brillouin scattering in hollow-core photonic bandgap fibers, New J. Phys. **18**, 025008 (2016).

[36] R. O. Behunin, Y.-H. Ou, and K. Kieu, Spontaneous forward Brillouin scattering in carbon disulfide, Phys. Rev. A **99**, 063826 (2019).

[37] E. A. Kittlaus, H. Shin, and P. T. Rakich, Large Brillouin amplification in silicon, Nat. Photon. **10**, 463 (2016).

[38] H. Shin, J. A. Cox, R. Jarecki, A. Starbuck, Z. Wang, and P. T. Rakich, Control of coherent information via on-chip photonic–phononic emitter–receivers, Nat. Commun. **6**, 6427 (2015).

[39] Y. Zhang, L. Wang, Z. Cheng, and H. K. Tsang, Forward stimulated Brillouin scattering in silicon microring resonators, Appl. Phys. Lett. **111**, 041104 (2017).

[40] G. Bahl, K. H. Kim, W. Lee, J. Liu, X. Fan, and T. Carmon, Brillouin cavity optomechanics with microfluidic devices, Nat. Commun. **4**, 1994 (2013).

[41] G. Bahl, J. Zehnpfennig, M. Tomes, and T. Carmon, Stimulated optomechanical excitation of surface acoustic waves in a microdevice, Nat. Commun. **2**, 403 (2011).

[42] J. Yu, Z. Shen, Z. Yang, S. Qi, Y. Jiang, G. Brambilla, C.-H. Dong, and P. Wang, The investigation of forward and backward Brillouin scattering in high-Q chalcogenide microspheres, IEEE Photon. J. **14**, 1 (2022).

[43] L. Dupays and J.-C. Pain, Closed forms of the Zassenhaus formula, J. Phys. A: Math. Theor. **56**, 255202 (2023).

[44] M. Gehl, D. Trotter, A. Starbuck, A. Pomerene, A. L. Lentine, and C. DeRose, Active phase correction of high resolution silicon photonic arrayed waveguide gratings, Opt. Express **25**, 6320 (2017).

[45] K. Takada, M. Abe, T. Shibata, and K. Okamoto, 1-GHz-spaced 16-channel arrayed-waveguide grating for a wavelength reference standard in DWDM network systems, J. Lightwave Technol. **20**, 850 (2002).

[46] See Supplemental Material at http://link.aps.org/supplemental/10.1103/z8tj-ml6k for Heralding fidelity.

[47] P. Meystre, Quantum optics: Taming the quantum, *Graduate Texts in Physics* (Springer International Publishing, Cham, 2021).

[48] M. Aspelmeyer, T. J. Kippenberg, and F. Marquardt, Cavity optomechanics, Rev. Mod. Phys. **86**, 1391 (2014).

[49] M. Puckett, D. Bose, K. Nelson, and D. J. Blumenthal, Higher order cascaded SBS suppression using gratings in a photonic integrated ring resonator laser, in *Proceedings of the Conference on Lasers and Electro-Optics (CLEO)* (Optical Society of

America / Optica, 2010 Massachusetts Ave. NW, Washington, DC, USA, 2019), pp. 1–2.

[50] M. Wang, Z.-G. Hu, C. Lao, Y. Wang, X. Jin, X. Zhou, Y. Lei, Z. Wang, W. Liu, Q.-F. Yang, and B.-B. Li, Taming Brillouin optomechanics using supermode microresonators, Phys. Rev. X **14**, 011056 (2024).

[51] K. Liu, N. Chauhan, M. Song, M. W. Harrington, K. D. Nelson, and D. J. Blumenthal, Tunable broadband two-point-coupled ultra-high-Q visible and near-infrared photonic integrated resonators, Photon. Res. **12**, 1890 (2024).

[52] K. Liu, J. Wang, N. Chauhan, M. W. Harrington, K. D. Nelson, and D. J. Blumenthal, Integrated photonic molecule Brillouin laser with a high-power sub-100-mHz fundamental linewidth, Opt. Lett. **49**, 45 (2024).

[53] H. Lee and G. P. Agrawal, Suppression of stimulated Brillouin scattering in optical fibers using fiber Bragg gratings, Opt. Express **11**, 3467 (2003).

[54] M. Merklein, I. V. Kabakova, T. F. S. Büttner, D.-Y. Choi, B. Luther-Davies, S. J. Madden, and B. J. Eggleton, Enhancing and inhibiting stimulated Brillouin scattering in photonic integrated circuits, Nat. Commun. **6**, 6396 (2015).

[55] M. J. Holland and K. Burnett, Interferometric detection of optical phase shifts at the Heisenberg limit, Phys. Rev. Lett. **71**, 1355 (1993).

[56] A. Ourjoumtsev, H. Jeong, R. Tualle-Brouri, and P. Grangier, Generation of optical 'Schrödinger cats' from photon number states, Nature (London) **448**, 784 (2007).

[57] X. Zou and W. Mathis, Generating a four-photon polarization-entangled cluster state, Phys. Rev. A **71**, 032308 (2005).

[58] I. Dhand, M. Engelkemeier, L. Sansoni, S. Barkhofen, C. Silberhorn, and M. B. Plenio, Proposal for quantum simulation via all-optically-generated tensor network states, Phys. Rev. Lett. **120**, 130501 (2018).

[59] J. L. O'Brien, A. Furusawa, and J. Vučković, Photonic quantum technologies, Nat. Photon. **3**, 687 (2009).

[60] N. Gisin and R. Thew, Quantum communication, Nat. Photon. **1**, 165 (2007).

[61] P. Kok, W. J. Munro, K. Nemoto, T. C. Ralph, J. P. Dowling, and G. J. Milburn, Linear optical quantum computing with photonic qubits, Rev. Mod. Phys. **79**, 135 (2007).

[62] S. Chen, Y.-A. Chen, T. Strassel, Z.-S. Yuan, B. Zhao, J. Schmiedmayer, and J.-W. Pan, Deterministic and storable single-photon source based on a quantum memory, Phys. Rev. Lett. **97**, 173004 (2006).

[63] D. N. Matsukevich, T. Chanelière, S. D. Jenkins, S.-Y. Lan, T. A. B. Kennedy, and A. Kuzmich, Deterministic single photons via conditional quantum evolution, Phys. Rev. Lett. **97**, 013601 (2006).